Available online at www.elixirpublishers.com (Elixir International Journal)

Electrical Engineering

Elixir Elec. Engg. 54A (2013) 12793-12798

ISSN: 2229-712X

Simulation of single phase boiling in a rectangular duct according to IC engines operating conditions

Reza Hemmat Khanlou, Arash Mohammadi and Sayed Ali Jazayeri

K.N.Toosi University of Technology, Pardis Ave.,Molasadra St, Tehran, Iran.

ARTICLE INFO

Article history:

Received: 16 July 2012;

Received in revised form:

15 March 2013;

Accepted: 18 March 2013;

Keywords

Heat transfer,

Sub-cooled boiling,

IC engine cooling.

ABSTRACT

Rising demands on engine performance, fuel consumption, emission, etc. leads to study thermal behavior of cooling system in engines precisely. To minimize the time of 3-D numerical simulation, single phase boiling approach was used. Sub-cooled boiling heat transfer consists of two components (i.e. forced convection and boiling). The convective component is evaluated from flow analyses and to evaluate boiling heat transfer, two popular models, Chen and BDL, are considered. To study sub-cooled boiling heat transfer in engine cooling passages, a rectangular, bottom-heated, horizontal duct is simulated here to assess the effects of different working conditions (i.e. pressure, velocity and coolant type) on heat transfer. Comparing the numerical results with the experimental ones reveals that Chen model is more precise than BDL in predicting boiling heat transfer in engine cooling system.

© 2013 Elixir All rights reserved.

Introduction

Conventionally, IC engine cooling systems are designed to utilize the forced convection heat transfer regime with no excursions into the vapor phase [1,2]. However, there is evidence that many engines experience a degree of sub-cooled nucleate boiling from hot surfaces under some operating conditions. Boiling is an extremely advantageous mechanism, due to its ability to extract higher rates of heat transfer for only small increases in wall temperatures. A considerable reduction in fuel consumption and exhaust emission would be expected if a boiling regime is properly utilized in the development of modern cooling systems of IC engines [3].

When the engine is running, a coolant liquid flows and circulates within water cooling passages in the block and head. It carries away excess heat generated from the hotter wall in order to maintain normal operation of engine. Heat transfer has two kinds of forms in the cooling passages of a high power intensity engine: forced convection and flow boiling heat transfer. Fig. (1) shows a schematic which illustrates important locations and regions of the process of heat transfer in cooling passages. When the engine starts running, the wall temperature and the bulk liquid temperature are below the local saturation temperature. Under a constant heat flux wall boundary condition, the wall temperature rises linearly and is parallel to the bulk liquid temperature. At location B, the wall temperature reaches the saturation temperature of the liquid. Because of the hysteresis effect of boiling phenomenon, bubbles do not occur immediately as a certain amount of wall superheat is needed to nucleate cavities existing on the wall. Until at the point C, the first bubbles appear on the wall identified as ONB (Onset of Nucleate Boiling). So heat transfer type is based mainly on single-phase forced convection between A and C. Between the points C and D, many nucleation sites are activated and the bubbles either adhere on the hot surface or disappear in the bulk fluid as moving downstream. And then the wall temperature begins to level off. The contribution to heat transfer from the boiling continues to rise while the convective contribution diminishes.

This region is called PDB (Partial Developed Boiling). At E, the convective contribution becomes insignificant and FDB (Fully Developed Boiling) is established. Subsequently, the wall temperature remains almost constant or appreciably decreases in the FDB region while the bulk temperature reaches to the saturation temperature. Farther downstream, the heat transfer entered into the saturated flow boiling stage. Generally, the coolant temperature should be controlled below the saturated temperature. In other word, the boiling heat transfer process in water jacket belongs to the category of sub-cooled flow boiling heat transfer (before E).

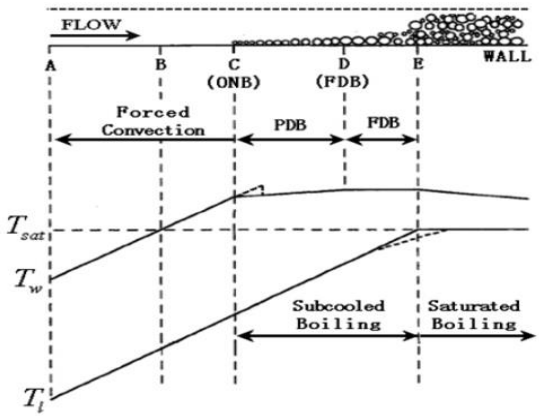

Fig.1 Process of heat transfer of sub-cooled flow boiling

Therefore, this paper has mainly taken some research in the sub-cooled flow boiling heat transfer.

Mathematical Formulation of the sub-cooled boiling flow model

Many models suggested for sub-cooled flow boiling assume the total wall heat flux q_w to be superimposed of two additive contributions, which can be written as

Tele:

E-mail addresses: Reza_hemmatkhanlou@sina.kntu.ac.ir

© 2013 Elixir All rights reserved

$$q_w = q_{fc} + q_{nb} \quad (1)$$

The first term q_{fc} is due to forced convection, the latter q_{nb} is due to nucleate boiling.

Among the superposition models, the model (Eq. 2) proposed by Chen [4] is widely used today especially in engineering applications in the automotive industry.

$$q_w = q_{fc}\varphi + q_{nb}S \quad (2)$$

Where the two correction parameters φ and S modify the forced convection heat flux q_{fc} and nucleate boiling heat flux q_{nb}, respectively. Both heat fluxes are computed following Chen's proposal. Accordingly, the first is written as

$$q_{fc} = h_{fc}(T_w - T_b) \quad (3)$$

Where the heat transfer coefficient h_{fc} is calculated using the Dittus-Boelter equation

$$Nu_{fc} = \frac{h_{fc}\, d_{hyd}}{\lambda_l} = 0.023 Re_l^{0.8} Pr_l^{0.4} \quad (4)$$

Involving the bulk flow Reynolds number and the Prandtl number of the liquid phase.

$$Re_l = \frac{\rho_l u_b d_{hyd}}{\mu_l}, \qquad Pr_l = \frac{\mu_l c_{p,l}}{\lambda_l}$$

respectively.

The factor φ occurring in Eq. (2) represents the enhancement of the convective component due to bubble agitation. Chen [4] derived a graphic relationship for φ as a dependent of the inverse of the Martinelli number X_{tt}, which reads

$$\left(\frac{1}{X_{tt}}\right) = \left(\frac{\xi_g}{1-\xi_g}\right)^{0.9}\left(\frac{\rho_l}{\rho_g}\right)^{0.5}\left(\frac{\mu_g}{\mu_l}\right)^{0.1} \quad (5)$$

Where ξ_g denotes mass fraction of the vapour. Butterworth [5] fitted this relationship $\varphi = \varphi\left(\frac{1}{X_{tt}}\right)$ with

$$\xi_g > 0: \quad \varphi = 2.35\left(\frac{1}{X_{tt}} + 0.213\right)^{0.736} \quad (6)$$

$$\xi_g \le 0.1: \quad \varphi = 1$$

In sub-cooled boiling flow the vapor mass fractions are typically small, such that $\xi_g \le 0.1$ applies and φ can be assumed unity.

The nucleate boiling heat flux

$$q_{nb} = h_{fc}(T_w - T_s) \quad (7)$$

is obtained using a correlation due to Forster and Zuber [6]

$$h_{nb} = 0.00122 \frac{\lambda_l^{0.79} c_{p,l}^{0.45} \rho_l^{0.49}}{\sigma^{0.5} \mu_l^{0.29} h_{lg}^{0.24} \rho_g^{0.24}} \Delta T_{sat}^{0.25} \Delta p_{sat}^{0.75} \quad (8)$$

Where the saturation pressure difference corresponding to the superheat temperature is written as

$$\Delta p_{sat} = p_{sat}(T_w) - p_{sat}(T_{sat})$$

The essential difference between Chen's approach and the BDL is in the modeling of the modification of the nucleate boiling component in terms of the factor S in Eq. (2). Chen introduced this parameter S as a flow-induced suppression factor, which he correlated as an empirical function of the product $Re_l \varphi^{1.25}$. This correlation was later fitted by Butterworth [5] with the expression

$$S_{Chen} = \frac{1}{1 + 2.53 \times 10^{-6} (Re_l \varphi^{1.25})^{1.17}} \quad (9)$$

For sub-cooled boiling flow, where $\varphi \approx 1$, the factor S_{Chen} obviously depends on the bulk flow Reynolds number only.

In some texts, S_{Chen} is stated as following

$$S_{Chen} = 1 \qquad Re < 1.10^4$$
$$S_{Chen} = 3.4 - 0.6\log(Re) \qquad 1.10^4 \le Re \le 4.10^5$$
$$S_{Chen} = 3.876 \times 10^{-2} \qquad Re > 4.10^5$$

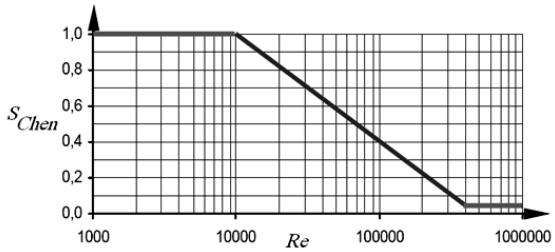

Fig. 2 Chen Suppression Factor

The Chen model provides a good description of the wall heat transfer enhancement due to nucleate boiling. Meanwhile it does not provide a correct description of the heat flux saturation that occurs when ΔT_{sat} increases and the fluid enters in the transition boiling region. In that case, the Chen correlation predicts a continuously increasing heat flux instead of the physical saturation.

The main deficiency of Chen model is located on the suppression factor. As a function of a Reynolds number of the global geometry, it cannot take the local fluid state into account. In particular, the effect of heat flux saturation while approaching the boiling transition region cannot be predicted.

The Boiling Departure Lift-off model is a recent improvement [7] in which the suppression factor is computed from local velocity and length scales.

In the BDL model the suppression factor is decomposed in two parts

$$S_{BDL} = S_{BDL1} S_{BDL2} \quad (10)$$

First suppression factor

The modeling of the first suppression factor S_{BDL1} is based on the study of bubble growth and dynamics [8]. Fig. (3) describes the process

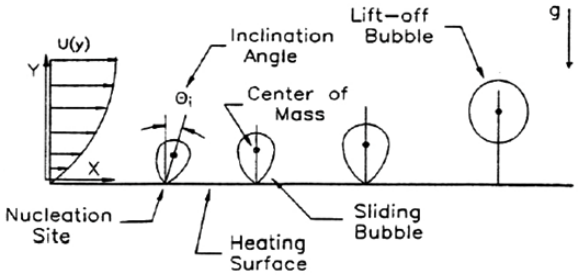

Fig. 3 Bubble Departure and Lift-off

This study assumes that the wall is horizontal.

When a bubble is generated on the wall, it starts to grow on a fixed wall point called the *nucleation site*. The set of forces applied on the bubble gives it a droplet shape with the axis slightly inclined downstream. The angle of the axis with the vertical is θ.

Once the bubble diameter is big enough, the bubble starts to slide downstream along the wall though is still attached to the wall. This diameter is called the *Departure Diameter* d_D.

While sliding, the bubble axis comes back to the vertical and the bubble still grows until its diameter is big enough to allow the bubble to leave the wall. This is the Lift-off and the corresponding diameter is called the *Lift-off Diameter* d_L.
The first suppression factor is then defined as:

$$S_{BDL1} = \left(\frac{d_D}{d_L}\right)^n \quad (11)$$

Where the exponent n has been calculated from model calibration.

Departure and Lift-off Diameters

Fig. (4) shows the forces influencing the bubble growth (some other forces exist but they are negligible). These forces are:

- The growth force F_{du}:

$$F_{du} = -\rho_l(T_{sat})4b^4 Ja^4\left(\frac{\lambda}{\rho_l C_p}\right)^2 \frac{1}{\pi}\left(\frac{3}{2}C_s - 1\right) \quad (12)$$

Where the Jakob number is defined as:

$$Ja = \frac{\rho(T_{sat})c_p(T_{sat})(T_w - T_{sat})}{\rho_v(T_{sat})L_v(T_{sat})} \quad (13)$$

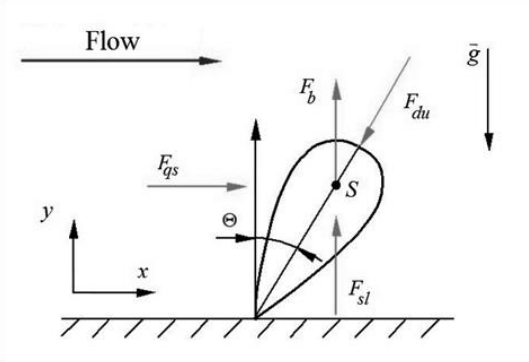

Fig. 4 Forces applied on a bubble

- The buoyancy force F_{bcy}:

$$F_{bcy} = \frac{4}{3}\pi r^3\left(\rho_l(T_{sat}) - \rho_v(T_{sat})\right)g \quad (14)$$

Where g is the gravity acceleration and r the bubble radius.

- The quasi-steady drag force F_{qs}:

$$F_{qs} = 6\pi\rho_l(T_{sat})\frac{\mu_l}{\rho_l}u_r r\left[\frac{2}{3} + \left[\left(\frac{12}{Re_{bub}}\right)^m + 0.796^m\right]^{-\frac{1}{m}}\right] \quad (15)$$

Where u_r is the velocity at the bubble center and Re_b is the bubble Reynolds number. The bubble velocity is estimated

- The shear lift force F_{sl}:

$$F_{sl} = \frac{1}{2}\rho_l u_r^2 \pi r^2 3.877\sqrt{G_s}\left(\frac{1}{Re_{bub}^2} + 0.014G_s^2\right)^{0.25} \quad (16)$$

Where G_s is the shear rate.
When the bubble starts to slide on the wall, it is assumed that its velocity is the same as the liquid around. Therefore the bubble velocity u_r and the velocity gradient in the shear rate G_s are estimated due to the Reichart law of the wall.

The departure diameter is then calculated as the root of the force balance.

When the bubble lifts-off the bubble main axis is vertical $(\theta = 0)$ and so is its motion. Therefore the bubble streamwise velocity u_r is zero and so are the quasi-steady force F_{qs} and shear lift force F_{sl}. The lift-off diameter d_L is then obtained from the force balance under the previous conditions.

Second Suppression Factor

The second suppression factor is a correction to the definition of the pool boiling coefficient h_{pool}. In the Eq. (4) the temperature and pressure differences refer to the wall temperature while the bubble center is not exactly on the wall. As shown in Fig. (5) the correct relation should be:

$$h_{pool} = 0.00122\left[\frac{C_p^{0.45}\lambda^{0.79}\rho_l^{0.49}}{L_v^{0.24}\rho_v^{0.24}\sigma^{0.5}\mu^{0.29}}\right]\Delta T_{eff}^{0.24}\Delta P_{eff}^{0.75} \quad (17)$$

With ΔT_{eff} and ΔP_{eff} referring to the bubble center temperature.
These considerations give rise to the derivation of S_{BDL2}:

$$S_{BDL2} = \frac{S_{BDL1}h_{pool}}{1 + C_{BDL}Nu} \quad (18)$$

Where Nu is a bubble Nusselt number.

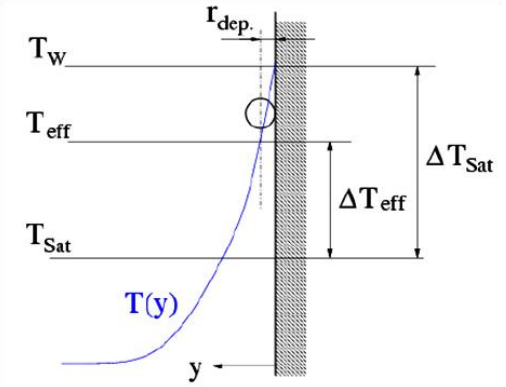

Fig. 5 Definition of effective temperature and pressure

Validation Case

The experimental data from Robinson's work [2] were used to validate the models for the variation of heat transfer rate versus the changes of the wall temperature under different pressures, flow velocities and coolant types. The measured data were obtained from a cooling gallery simulator rig designed to simulate the condition of engine coolant flow with nucleate boiling. As shown in Fig. (6), the channel is horizontal, 241 mm long and has a rectangular cross section of .The heating surface is at the bottom of the flow channel, located 76 mm downstream from the entrance of the channel. The test sample was machined from aluminum alloy (AS10G) used for cylinder head castings. The distribution of temperature and heat flux across the heating surface were claimed as uniform. The coolant fluid used in the experiment was a mixture of 50% ethylene glycol antifreeze and 50% water (by volume). A schematic diagram of the test section is shown in Figures (7) and (8). Traversing thermocouples, developed by Ricardo were incorporated into the test pieces. At all three locations shown, the thermocouples were traversed along the heat flow axis to within 2 mm of the heat transfer surface. The heat flux at each point was evaluated as the product of the temperature gradient and metal thermal conductivity, while the surface temperature was calculated by a small extrapolation of the temperature gradient. The fluid flow was considered to be fully turbulent under the experimental conditions outlined above and was modeled using the $k-\varepsilon$ turbulent model in conjunction with the wall function approach. A 3D mesh containing hexagonal elements was generated covering the entire flow domain. A uniform distribution of the

inlet velocity and temperature as well as the outlet pressure was defined according to the measured bulk data and a uniform temperature distribution was defined in the heating surface, while other walls were assumed to be adiabatic.

The precision of boiling models including Chen and BDL are compared within the CFD framework by validation against experimental data from Robinson's work [2] in a horizontal duct according to the IC engine operating conditions.
Computations are performed on the CFD code AVL Fire.

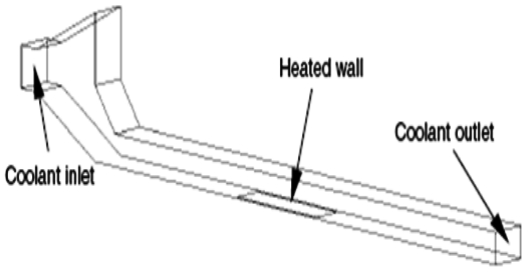

Fig. 6 Geometry of the flow channel

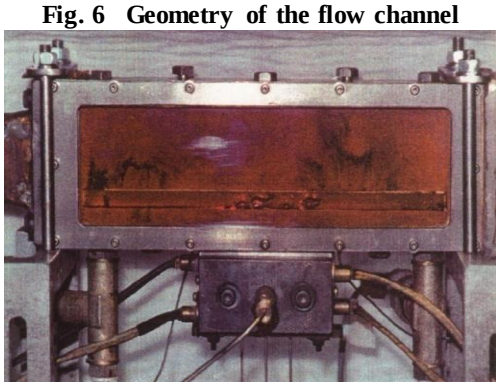

Fig. 7 Close-up view of the test duct of the engine cooling gallery simulator

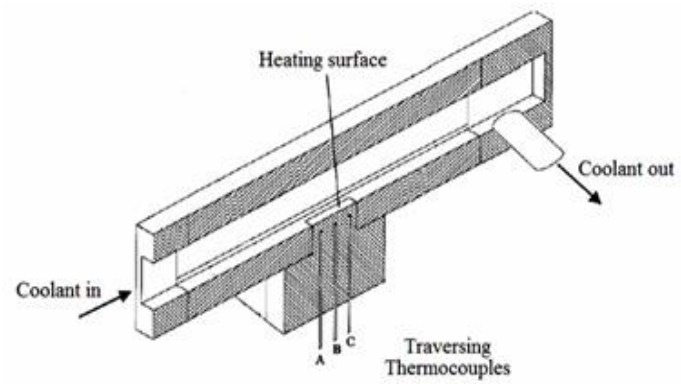

Fig. 8 Cutaway diagram of the rig duct and the traversing thermocouples position

Comparison of model predictions with experiments

Nine groups of data from test series were selected for the validations are summarized in table 1. Pressure is varied from group 1 to 3 and from 4 to 6, each at a fixed bulk flow velocity of liquid. The flow velocity is varied in groups 4,5,6 with respect to groups 1,2,3. Groups 7 to 9 describe a change in coolant type.

For each data point, the inlet/outlet mass flow in the CFD simulation was specified in the way that the bulk coolant flow velocity matches with the measured value pressure and temperature at the inlet were also specified according to test conditions. On the heated wall a constant temperature condition was applied. The rest of the walls were assumed to be adiabatic. The CFD calculation returns heat fluxes on the heat wall.

Table 1 Summary of data test used for validation

Groups No.	Pres.(bar)	Vel.(m/s)	T_inlet('C)	Coolant(Glycol Volume Fraction%)
1	1	0.25	90	50
2	2	0.25	90	50
3	3	0.25	90	50
4	1	1	90	50
5	2	1	90	50
6	3	1	90	50
7	2	0.25	90	(pure water)
8	2	0.25	90	50
9	2	0.25	90	(pure E.G.)

Figures (9) and (10) show the comparison of measured heat flux through the heated wall versus wall temperature under different pressures at bulk coolant velocity of 0.25 m/s and 1 m/s.

The most important effect of pressure on the boiling heat transfer is through its close association with the saturation temperature. When the inlet and wall boundary conditions are given, the saturation temperature determines the degree of superheating ΔT_{SUP} and sub-cooling ΔT_{SUB}, and hence the onset and the intensity of boiling. Boiling temperatures associated with pressures of 1 bar, 2 bar and 3 bar are $110.5^{\circ}C$, $128^{\circ}C$ and $142^{\circ}C$ respectively. It's expected that before the wall temperature reaches the saturation point, the wall heat flux increases linearly with the wall temperature, exhibiting the feature of a constant heat transfer coefficient under the non-boiling condition. After the wall temperature exceeds the saturation point, the heat flux increases rapidly as the results of the onset of nucleate boiling.

According to table (1) working conditions the results are compared in Figures 9-11 With experiments. To demonstrate the effect of liquid properties, simulations were repeated for 3 coolants with different Ethylene Glycol volume fractions. It is seen that when the flow and thermal boundary conditions are the same, the heat transfer rate is much higher with water as the working fluid than coolant. The difference is mainly due to change of saturated temperature.

Overall from Fig. 12 (a to i) the agreement between CFD predictions and the measurement is satisfactory, although some discrepancy exists. Except the fact that the model is simple and therefore may not effectively cover all the possible mechanisms involved in the nucleate boiling heat transfer, the discrepancy could also come from either inaccuracy of coolant properties used in CFD calculation or experimental errors.

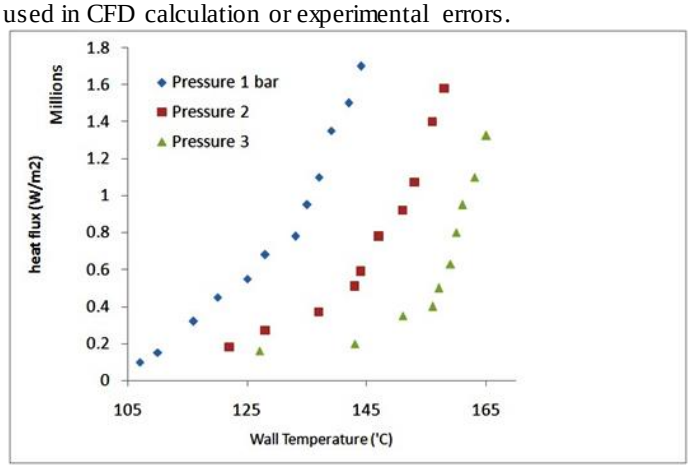

Fig. 9 Experimetal data of groups 1-3

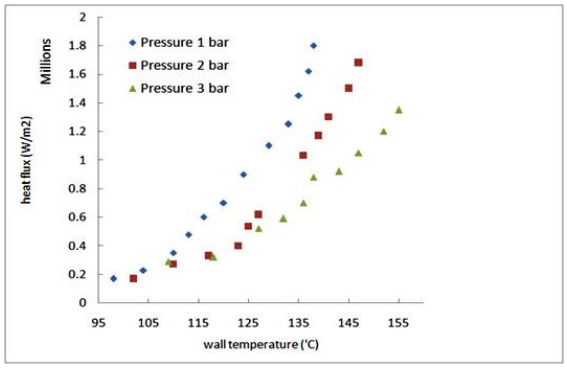

Fig.10 Experimental data of groups 4-6

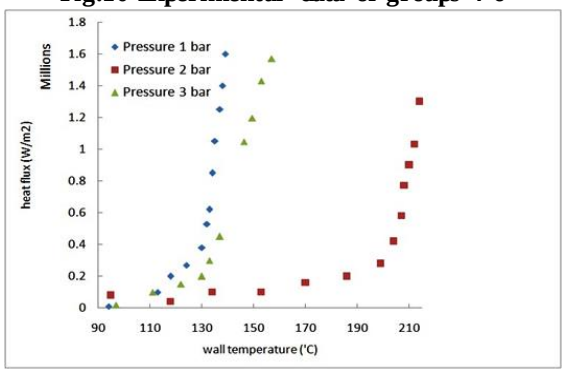

Fig. 11 Experimental data of groups 7-9

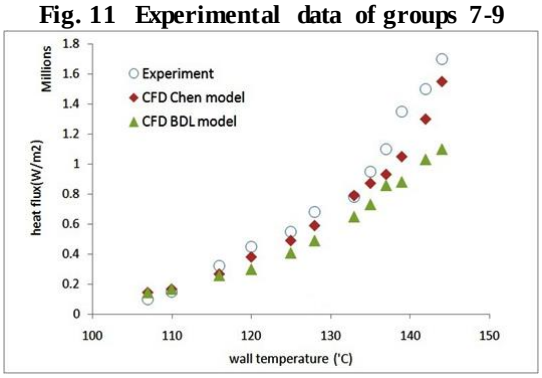

a) group 1

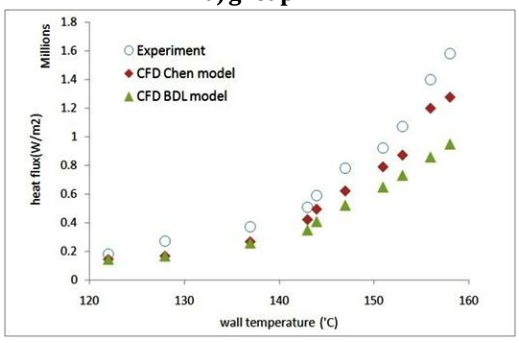

b)group 2

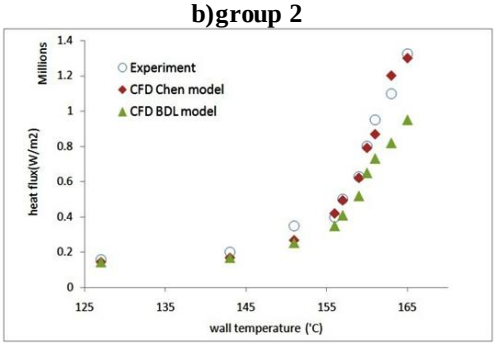

c) group 3

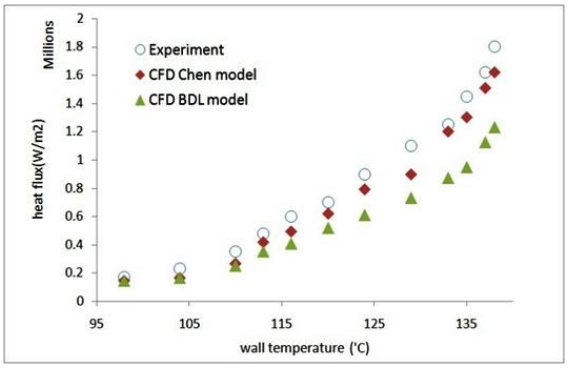

d)group 4

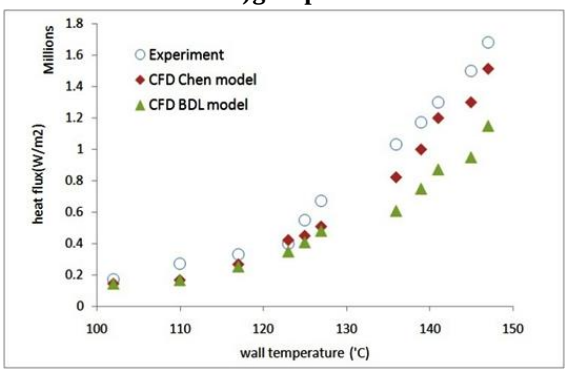

e) group 5

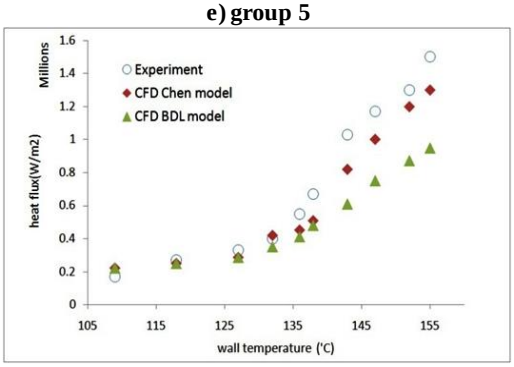

f) group 6

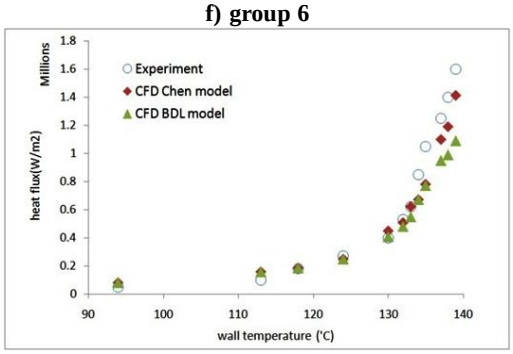

g)group 7

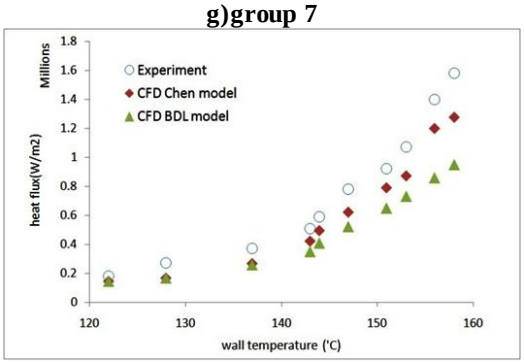

h)group

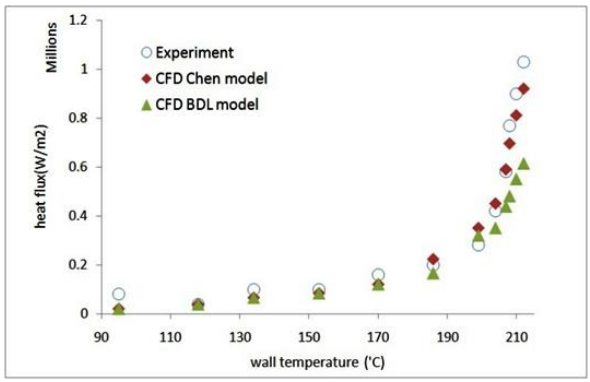

i) group 9

Fig.12 Comparison of models and experiments of groups 1-9

Conclusion

Comparison between experiments and predicted data reveals that the two proposed model, Chen and BDL, have got good agreement with the experimental results. But as seen obviously, Chen model predicts nucleate boiling more precise than BDL model in IC engine's operating conditions.

Nomenclature

b model constant [-]
c specific heat [$J/kg\,K$]
C_s constant [-]
D diameter [m]
d_{hyd} hydraulic diameter [m]
F force [N]
g gravitational acceleration [m/s^2]
h heat transfer coefficient [W/m^2K]
Ja jakob number[-]
L_v latent heat [J/kg]
m constant [-]
Nu nusselt number [-]
P pressure [N/m^2]
Pr prandtl number [-]
q specific heat transfer rate [W/m^2]
r radius [m]
Re Reynolds number [-]
S suppression factor [-]
T temperature [C]
t time [s]
u velocity [m/s]
x axial coordinate [m]
X_{tt} Martinelli number[-]
y wall normal coordinate [m]

Greek symbols

μ dynamic viscosity[kg/ms]
ρ mass density [kg/m^3]
φ correction parameter [-]
λ conductivity [W/mK]
σ surface tension [kg/s^2]
θ inclination angle [rad]
ξ mass fraction [-]

Subscripts

b bulk
bcy buoyancy
bub bubble
du bubble growth
D departure
eff effective
fc forced convection
FDB fully developed boiling
g vapor phase
l liquid phase
L lift-off
nb nucleate boiling
p constant pressure
PDB partially developed boiling
sat saturated
sl shear lift
sub sub-cooling
w wall

References

[1]Kanefsky,P., Nelson, V. A. and Ranger, M. A systems engineering approach to engine cooling design. 44th Buckendale Lecture, SAE Congress, 1- 4 March 1999.

[2]Robinson, K. IC engine coolant heat transfer studies. PhD thesis, University of Bath, 2001.

[3]Dong,F., Fan,Q., Numerical simulation of boiling heat transfer in water jacket of DI engine, SAE 2010-01-0262

[4]J.C. Chen, A correlation for boiling heat transfer to saturated fluids in convective flow, ASME preprint 63 HT34 presented at the 6th National Heat Transfer Conference, Boston, 1963.

[5]D. Butterworth, the correlation of cross flow pressure drop data by means of a permeability concept, UKAEA Report AERE-R9435, 1979.

[6]H.K. Forster, N. Zuber, Dynamics of vapor bubbles and boiling heat transfer,AIChE J. 1 (1955) 531-535.

[7]Ablinger S., "*Kalibrierung und Verifikation von Siedemodellen fur die 3D-Stromungssimulation*", Diplomarbeit an der TU-Graz, 2002.

[8]Klasuner J.F., Zeng L.Z., Bernhard D.M., Mei R., "A unified model for the prediction of bubble detachment diameters in boiling systems-II. Flow boiling". Int. I. Heat Mass Transfer, Vol.36, No.9, pg.2271-2279, 199.